# Coupled Longitudinal and Lateral Control for an Autonomous Vehicle Dynamics Modeled Using a Robotics Formalism

Alia Chebly, R Talj, A. Charara

# Coupled Longitudinal and Lateral Control for an Autonomous Vehicle Dynamics Modeled Using a Robotics Formalism

**A. Chebly** * **R. Talj** * **A. Charara** *

* *Heudiasyc Laboratory, Sorbonne universités, Université de technologie de Compiègne, CNRS, Heudiasyc UMR 7253, CS 60 319, 60 203 Compiègne, France (e-mails: alia.chebly@hds.utc.fr reine.talj@hds.utc.fr ali.charara@hds.utc.fr)*

**Abstract:** The development of autonomous and intelligent vehicles is increasing continuously in the aim to reach a reliable and secured transportation system. Indeed, autonomous navigation include three main steps: perception and localization, planning and control. This work covers essentially the study of the vehicle modeling and the vehicle control. We present a coupled control algorithm for longitudinal and lateral dynamics of an autonomous vehicle. The control is realized using Lyapunov functions and aims to ensure a robust tracking of the reference trajectory especially in coupled longitudinal and lateral maneuvers such as lane-change maneuvers, obstacle avoidance maneuvers and combined lane-keeping and steering control during critical driving situations. The control is based on the vehicle model that is carried out using the robotics formalism. This modeling approach is considered here for the accuracy it presents, since multi-body models provide more information, which are usually neglected when using a closed-form model. It considers the vehicle as a multi-body poly-articulated system and uses the modified Denavit-Hartenberg geometric description to represent the vehicle. Newton-Euler algorithm is then used to compute the direct dynamical model of the vehicle. The developed model takes into consideration all the vehicle parts and their interconnections, that renders it more representative of the vehicle behavior especially in critical driving scenarios.

*Keywords:* Autonomous vehicles, coupled control, maneuvers tracking, vehicle modeling, robotics formalism, robustness.

## 1. INTRODUCTION

The development of autonomous vehicles has received a lot of attention during the last decades. The motivation is to guarantee a reliable and secure vehicle navigation even in critical driving situations. Actually, an autonomous system can react faster than a human driver, which will diminish the road accidents often caused by the driver's mistakes. Several challenges, such as the DARPA challenge in the USA (Buehler et al. (2009)), the GCDC 2016 challenge in the Netherlands, and many others have been organized all around the world to favor this research field. Indeed, an autonomous navigation can be completed in three key steps: the perception and localization, the path planning and the vehicle control. In this work, we focus on the vehicle modeling and the vehicle coupled control.

A four wheels vehicle model is developed using robotics formalism based on the modified Denavit-Hartenberg parameterization. We propose after that a combined vehicle control scheme to cope with driving situations involving average longitudinal speeds and coupled longitudinal/lateral maneuvers. Actually, the vehicle modeling is a key step for control objectives since it permits to better understand and illustrate the vehicle dynamics. Hence, the goal is to build a mathematical model that illustrates the significant aspects of the physical dynamics and then facilitates the performance analysis. Most of the models proposed in the literature are developed for control applications (Sharp (1971)). Lately, some advanced models have been developed using multi-body systems to model a complex system (Kiencke and Nielsen (2000); Rajamani (2006)). In this work, we proceed in a systematic geometrical description, based on the modified Denavit Hartenberg parametrization (Khalil and Kleinfinger (1986)). The modeling is then conducted by applying recursive methods used in robotics, more precisely, recursive Newton-Euler based Algorithm (Khalil and Kleinfinger (1987)). This description allows to compute, directly, the symbolic expression of the geometric, kinematic and dynamic models of the vehicle. The motivation to use this approach is the fact that it permits to elaborate systematically the symbolic equations of motion and makes the implementation of the dynamic model easier. Moreover, multi-body models usually provide more information than the classical closed-forms model and are able for an easy manipulation (For example, we can simply modify some assumptions such as the presence or not of dampers or suspensions...).

The developed dynamic model is then used to elaborate a coupled control for the vehicle. In fact, the vehicle dynamics control has been widely discussed in the literature and several studies on longitudinal and lateral control have been conducted. However, the longitudinal and the lateral

controllers are addressed separately in the majority of cases. For lane keeping, lane-change maneuvers, pedestrian and obstacle avoidance, a lateral control is used (Ackermann et al. (1995); Rajamani et al. (2000); Tagne et al. (2013)). While, for adaptive cruise control and platooning tasks, the longitudinal control is developed (Rajamani et al. (2000); Mammar and Netto (2004)). Unfortunately, many critical driving situations involving the safe handling of vehicles require coupled control, and, such a strategy is rarely addressed in the literature. We are interested in this work by the combined control for the lateral and the longitudinal vehicle dynamics. The developed controller is based on the Lyapunov control techniques and aims to ensure a robust tracking of a reference trajectory given by a planning module. The reference trajectory is defined by a set of desired longitudinal velocities and desired curvatures to track. The paper is organized as follows: Section 2 presents the vehicle modeling by describing the global method and its application to the vehicle system. The model is validated using the Scaner-studio simulator and the simulations results are then illustrated. Section 3 presents the developed controller by describing the lateral and the longitudinal controls and the simulation results that validate our controller. Section 4 concludes the paper and shows our future works.

## 2. VEHICLE MODELING

### *2.1 Methodology*

The system is modeled using the formalism of robotics based on the geometrical description of modified Denavit-Hartenberg (DHM) (Maakaroun (2011); Khalil and Dombre (2004)). This method considers that the vehicle is a multi-articulated system consisting of $n$ bodies wherein the chassis is the movable base and the wheels are the terminals. Each body is connected to its antecedent by a joint which represents a translational or a rotational degree of freedom. A body can be virtual or real; the virtual bodies are introduced to describe joints with multiple degrees of freedom or to introduce intermediate fixed frames (see Fig. 1).

Several recursive algorithms were used to obtain the dynamic model of a robot (Renaud (1975); Hollerbach (1980); Hooker and Margulies (1965)). In our work, we adopted the mixed Euler-Lagrange formalism since it allows to directly elaborate the dynamic model of the robot with minimum computation time. The mixed Euler-Lagrange model is obtained from two recurrences of the algorithm of Newton-Euler in the following way (Luh et al. (1980)): The forward recursive equations (from the mobile base to the effectors) compute the total forces ${}^jF_j$ and moments ${}^jMo_j$ on each link $j$ by calculating the angular and the linear speeds and accelerations of each body. The backward recurrence (from the effectors to the mobile base) computes the forces ${}^jf_j$ and the moments ${}^jmo_j$ exerted on each body by its antecedent taking into account the external forces applied to the robot.

The torque $\tau_j$ applied on the body $C_j$ is calculated by projecting, according to the type of the joint $j$, the vector of force ${}^jf_j$ or moment ${}^jmo_j$ on the axle of movement.

$$\tau_j = (\sigma_j {}^jf_j + \bar{\sigma_j} {}^jmo_j)^t {}^ja_j \quad (1)$$

where ${}^ja_j = [0\ 0\ 1]^t$, $\sigma_j = 1$ if the joint $j$ is translational and $\sigma_j = 0$ if the joint $j$ is rotational. If there is no degree of freedom between two frames that are fixed with respect to each other, we take $\sigma_j = 2$. The reader can refer to Maakaroun (2011) and Maakaroun et al. (2014) for more details.

The inverse dynamic model of a robot with a mobile base can be written as

$$\tau = f(q, \dot{q}, \ddot{q}, f_e) = A(q)\ddot{q} + H(q, \dot{q}) + J(q)f_e \quad (2)$$

where $\tau$ is the vector of the actuators torques or forces, $q$, $\dot{q}$ and $\ddot{q}$ are the vectors of positions, velocities and accelerations of all the joints including the variables of the chassis, and $f_e$ is the vector of external forces. $H$ is the vector of centrifugal, coriolis and gravity terms, $J$ is the jacobien matrix, $Jf_e$ is the vector of generalized efforts representing the projection of external forces and torques on the joint axis, and $A$ is the inertial matrix of the system. The direct dynamic model is then given by:

$$\ddot{q} = [A(q)]^{-1}(\tau - H(q, \dot{q}) - J(q)f_e). \quad (3)$$

Once the expression of $\tau$ is determined by the Newton-Euler algorithm, we can develop the direct dynamic model by calculating the matrices $A$, $H$ and $J$ as follows:

- The column $c_a$ of the matrix $A$ is computed by
$$A(:, c_a) = \frac{\partial \tau}{\partial \ddot{q}(c_a)}, \quad c_a \in [1, l], \quad (4)$$
where $l$ represents the number of degrees of freedom in the system which is the dimension of the vector $q$.
- The matrix $J$ is computed similarly by
$$J(:, c_j) = \frac{\partial \tau}{\partial f_e(c_j)}, \quad c_j \in [1, r_f], \quad (5)$$
where $r_f$ represents the dimension of the vector $f_e$.
- The matrix H is obtained using $H(q, \dot{q}) = \tau$ when $\ddot{q} = f_e = 0$. Then,
$$H = f(q, \dot{q}, 0, 0) \quad (6)$$

### *2.2 Four wheels vehicle model*

The developed model is composed of 21 bodies (Fig. 1,2) defined as follows:

- $C_0$ is a virtual body used to represent the initial speeds of the vehicle
- $C_1$ represents the chassis
- $C_2$, $C_3$, $C_8$, $C_{13}$, $C_{14}$ and $C_{18}$ are virtual bodies introduced as intermediate fixed frames
- $C_4$and $C_9$ are the front right and front left steering columns respectively
- $C_5$, $C_{10}$, $C_{15}$, $C_{19}$ are virtual bodies fixed to the four wheels by blocked joints
- $C_6$, $C_{11}$, $C_{16}$ and $C_{20}$ are the front right, front left, rear right and rear left wheels respectively
- $C_7$, $C_{12}$, $C_{17}$ and $C_{21}$ are virtual bodies fixed to the four wheels.

The eight virtual bodies fixed to the four wheels are introduced to indicate that the wheels are in rotation around their axes while maintaining their contact with the ground. So, the contact forces between the four wheels and the ground are computed in the frames of the virtual bodies $C_7$, $C_{12}$, $C_{17}$ and $C_{21}$, which are fixed to the virtual

bodies $C_5$, $C_{10}$, $C_{15}$ and $C_{19}$. The four bodies $C_6$, $C_{11}$, $C_{16}$ and $C_{20}$ are related to the four wheels and they represent the wheels rotation in their frames.

we consider 7 degrees of freedom, $q$=$[x\ y\ \psi\ \theta_{fl}\ \theta_{fr}\ \theta_{rl}\ \theta_{rr}]^t$, where $x, y$ and $\psi$ are the longitudinal position, the lateral position and the yaw angle of the vehicle computed in the vehicle frame $R_0$. $\theta_{ij}$ is the angular position of a wheel, where $ij$ stands for front right (fr), front left (fl), rear right (rr) and rear left (rl) wheels. $V_x = \dot{x}$ and $V_y = \dot{y}$ are the longitudinal and the lateral speeds of the vehicle computed in the vehicle frame, $w_{ij} = \dot{\theta}_{ij}$ is the angular velocity of a wheel. The geometric representation is given in Fig. 1.

The external forces applied to the vehicle model, which have the most significant impact on the vehicle dynamics, are the contact forces between the ground and the tires. Aerodynamic forces also have an effect on the vehicle behavior, particularly at high speed ($> 90Km/h$).
The aerodynamic force $F_{aero}$ is given by

$$F_{aero} = 1/2\ \rho_a\ c_d\ s\ \dot{x}^2, \tag{7}$$

where $\rho_a$ is the mass density of air, $c_d$ is the aerodynamic drag coefficient, $s$ is the frontal area of the vehicle which is the projected area of the vehicle in the direction of travel and $\dot{x}$ is the longitudinal vehicle velocity. The contact forces between the tires and the ground are modeled using Dugoff modelization (Dugoff et al. (1970)).

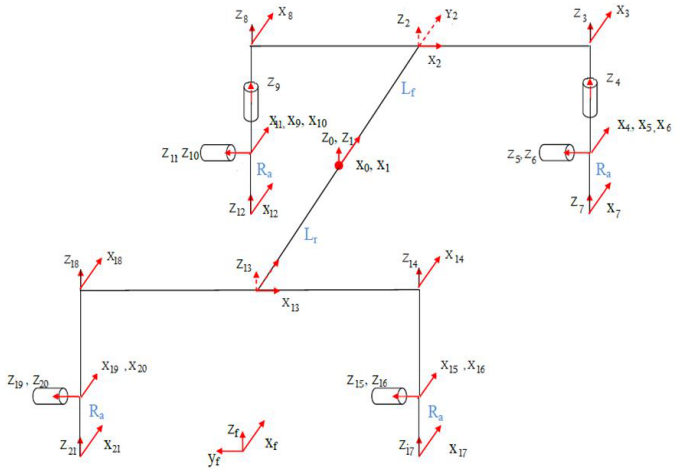

Fig. 1. Poly-articulated system with 21 bodies and 7 degrees of freedom.

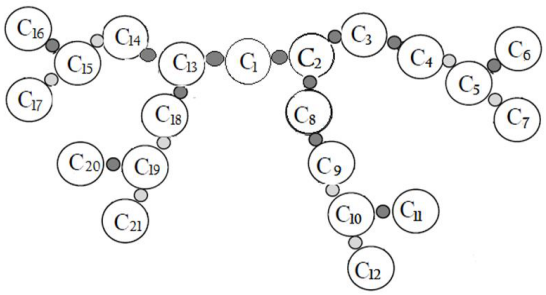

Fig. 2. Model topology with 21 bodies.

The developed dynamic model is then given by (3), where the matrices A, H and J are as follows:

$$A = \begin{pmatrix} m & 0 & 0 & 0 & 0 & 0 & 0 \\ 0 & m & -L_3 & 0 & 0 & 0 & 0 \\ 0 & -L_3 & I_3 & 0 & 0 & 0 & 0 \\ 0 & 0 & 0 & I_w & 0 & 0 & 0 \\ 0 & 0 & 0 & 0 & I_w & 0 & 0 \\ 0 & 0 & 0 & 0 & 0 & I_w & 0 \\ 0 & 0 & 0 & 0 & 0 & 0 & I_w \end{pmatrix} \tag{8}$$

$$H = \begin{pmatrix} 1/2\rho_a c_d s\dot{x}^2 - m\dot{\psi}\dot{y} + L_3\dot{\psi}^2 \\ m\dot{\psi}\dot{x} \\ -L_3\dot{\psi}\dot{x} \\ 0 \\ 0 \\ 0 \\ 0 \end{pmatrix} \tag{9}$$

and $J = [J_1\ J_2]$, where $J_1$ and $J_2$ are given by:

$$J_1 = \begin{pmatrix} -\cos(\delta_{fl}) & -\cos(\delta_{fr}) & -1 & -1 \\ -\sin(\delta_{fl}) & -\sin(\delta_{fr}) & 0 & 0 \\ -L_f\sin(\delta_{fl}) + t_r\cos(\delta_{fl}) & -L_f\sin(\delta_{fr}) - t_f\cos(\delta_{fr}) & t_r & -t_r \\ R_{eff} & 0 & 0 & 0 \\ 0 & R_{eff} & 0 & 0 \\ 0 & 0 & R_{eff} & 0 \\ 0 & 0 & 0 & R_{eff} \end{pmatrix}, \tag{10}$$

$$J_2 = \begin{pmatrix} \sin(\delta_{fl}) & \sin(\delta_{fr}) & 0 & 0 \\ -\cos(\delta_{fl}) & -\cos(\delta_{fr}) & -1 & -1 \\ -L_f\cos(\delta_{fl}) - t_r\sin(\delta_{fl}) & -L_f\cos(\delta_{fr}) + t_f\sin(\delta_{fr}) & L_r & L_r \\ 0 & 0 & 0 & 0 \\ 0 & 0 & 0 & 0 \\ 0 & 0 & 0 & 0 \\ 0 & 0 & 0 & 0 \end{pmatrix}, \tag{11}$$

The vectors $\tau$ and $f_e$ are given by:

$$\tau = \begin{pmatrix} 0\ 0\ 0\ \tau_{w_{fl}}\ \tau_{w_{fr}}\ \tau_{w_{rl}}\ \tau_{w_{rr}} \end{pmatrix}, \tag{12}$$

$$f_e = \begin{pmatrix} F_{x_{fl}}\ F_{x_{fr}}\ F_{x_{rl}}\ F_{x_{rr}}\ F_{y_{fl}}\ F_{y_{fr}}\ F_{y_{rl}}\ F_{y_{rr}} \end{pmatrix}. \tag{13}$$

The terms in $L_3$ and $I_3$ in (8) represent the interconnection between the different bodies composing the vehicle. Their presence makes the robotic approach more interesting, since it permits to develop a complete model of the vehicle showing the influence of each body on the other bodies. $L_3$ and $I_3$ are defined as

- $L_3$=$L_r(m_{rr} + m_{rl}) - L_f(m_{fl} + m_{fr})$,
- $I_3$=$I_z + t_f^2(m_{rl} + m_{rr} + m_{fr} + m_{fl}) + L_f^2(m_{fl} + m_{fr}) + L_r^2(m_{rr} + m_{rl})$

The parameters $m$, $I_w$, $L_f$, $L_r$, $I_z$ and $R_{eff}$ are defined in Table 2.2. $F_{x_{ij}}$ and $F_{y_{ij}}$ are the longitudinal and the lateral forces developed on the four wheels respectively, $m_{ij}$ is the mass of a wheel, $\delta_{fl}$ and $\delta_{fr}$ are the front left and the front right steering wheel angles and $\tau_{w_{ij}}$ is the driving/braking torque applied to the wheel with index (ij).

Table 1. Vehicle parameters

| | | |
|---|---|---|
| $m$ | Vehicle total mass | 1719 |
| $I_w$ | Rotational inertia of the wheel | 1.02 |
| $L_f$ | Distance between the COG and the front axle | 1.195 |
| $L_r$ | Distance between the COG and the rear axle | 1.513 |
| $m_{ij}$ | wheel mass | 12.2 |
| $I_z$ | Vehicle vertical inertia | 3300 |
| $R_{eff}$ | Effective radius of the tire | 0.316 |
| $C_\sigma$ | Longitudinal stiffness of a wheel | 80574 |
| $C_f$ | Cornering stiffness of a front wheel | 85275 |
| $C_r$ | Cornering stiffness of a rear wheel | 68922 |
| $t_f$ | Half front track of the vehicle | 0.7 |
| $t_r$ | Half rear track of the vehicle | 0.7 |

### 2.3 Model Validation Results

The algorithm was implemented under Matlab/Simulink and the model was validated using the Scaner-Studio simulator (Oktal (2016)). The model was validated for many navigation scenarios. We present below two scenarios: The first one shows a longitudinal acceleration scenario where the acceleration reaches $2.5m/s^2$ and the speed reaches $111Km/h$. The second scenario presents a big round about where the lateral acceleration reaches $3m/s^2$ and the speed varies between 11 and $40Km/h$.

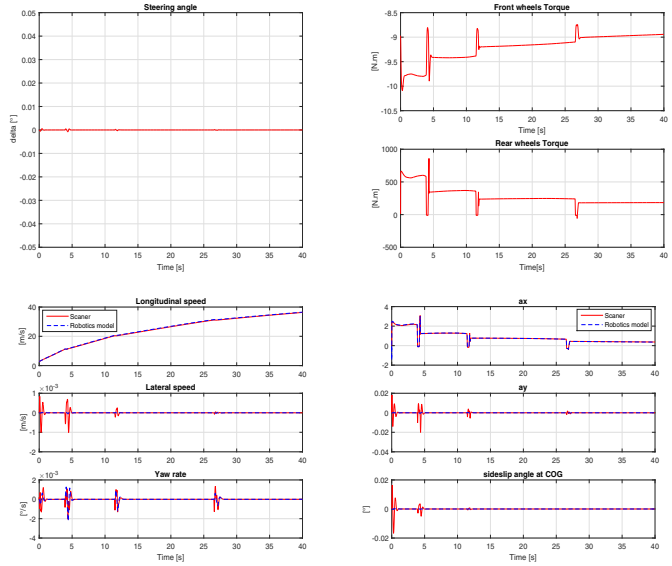


Fig. 3. First scenario: a) Steering angle, b) Wheels torque, c) speeds and yaw rate, d) accelerations and sideslip angle

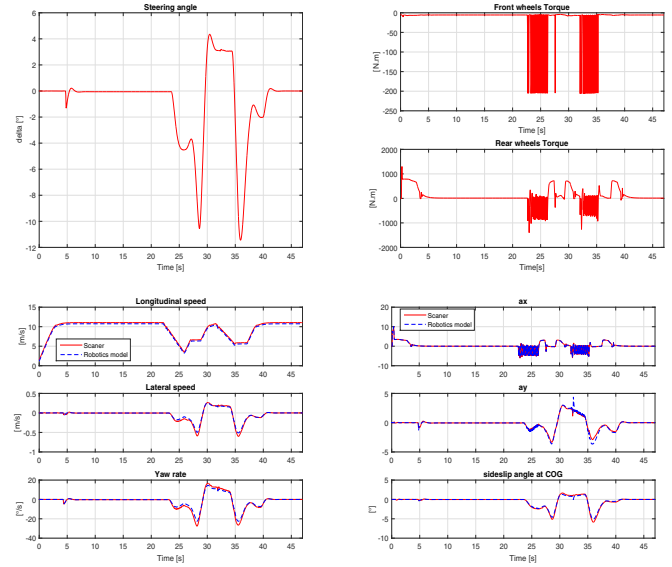


Fig. 4. Second scenario: a) Steering angle, b) Wheels torque, c) speeds and yaw rate, d) accelerations and sideslip angle

The model inputs which are the steering angle and the motor driving/braking torque are taken from the scenario conducted on Scaner-Studio. The model outputs, which are the vehicle dynamics variables, are compared to the outputs obtained by the simulator. Figure 3 presents the first scenario. The results presented in Figure 3c) and 3d) shows that the model outputs are so close to the simulator ones. Figure 4 shows the vehicle behavior in a round about, the vehicle decelerates while crossing the turn to attain $3m/s$. The results show that the model is representing the vehicle dynamics properly.

To conclude this section, we note that the developed model is valid in a large marge of driving conditions and can be used for control objectives. The next section of this paper presents the controller applied to this model. The controller theory is explained in detail and we present further more the validation results.

## 3. CONTROLLER DESIGN

### 3.1 Strategy

The objective of our controller is to ensure a robust tracking of the reference trajectory for any time varying maneuver. The tracking objective is reached by controlling the longitudinal velocity and the lateral displacement of the vehicle.

For more simplicity, the following assumptions are made:

- The longitudinal slip ratio is considered null, that renders $R_{eff}\dot{w}_{ij} = \ddot{x}$. Using this assumption in the wheels dynamics equations, we obtain: $F_{x_{ij}} = \frac{\tau_{w_{ij}}}{R_{eff}} - \frac{I_w \ddot{x}}{R_{eff}^2}$. ($ij$ is the wheel index as cited in section 2.2)
  A direct relation between the longitudinal acceleration of the vehicle and the motor torque is then obtained by replacing $F_{x_{ij}}$ in the first equation of the vehicle system (3).
- Only the rear wheels are motorized, so $\tau_{w_{fl}} = 0$ and $\tau_{w_{fr}} = 0$.
- The rear left and the rear right wheels receive the same torque, so $\tau_{w_{rl}} = \tau_{w_{rr}} = \frac{\tau_w}{2}$ ($\tau_w = \tau_{w_{fl}} + \tau_{w_{fr}}$).
- The estimation of the contact forces between the ground and the tires is based on the linear model (Baffet (2007)).
- The approximations of small angles are made.
- The front left and the front right wheels steering angles are supposed to be equal ($\delta_{fl} = \delta_{fr} = \delta$).

With all these assumptions, the vehicle model presented in Equation (3) can be rewritten as:

$$\begin{cases} m_e\ddot{x} - m\dot{y}\dot{\psi} + L_3\dot{\psi}^2 + F_{aero} = g_1, \\ m\ddot{y} + m\dot{x}\dot{\psi} - L_3\ddot{\psi} + 2C_f\dfrac{\dot{x}(\dot{y} + L_f\dot{\psi})}{\dot{x}^2 - (t_f\dot{\psi})^2} + 2C_r\dfrac{\dot{x}(\dot{y} - L_r\dot{\psi})}{\dot{x}^2 - (t_f\dot{\psi})^2} = g_2, \\ I_3\ddot{\psi} + 2L_fC_f\dfrac{\dot{x}(\dot{y} + L_f\dot{\psi})}{\dot{x}^2 - (t_f\dot{\psi})^2} - 2L_rC_r\dfrac{\dot{x}(\dot{y} - L_r\dot{\psi}))}{\dot{x}^2 - (t_f\dot{\psi})^2} = g_3, \end{cases} \tag{14}$$

where $m_e, g_1, g_2$ and $g_3$ are given by:

$$\begin{aligned} m_e &= m + 4\frac{I_w}{R_{eff}^2}, \\ g_1 &= \frac{\tau_w}{R_{eff}} - \delta(2C_f\delta - 2C_f\frac{\dot{x}(\dot{y} + L_f\dot{\psi})}{\dot{x}^2 - (t_f\dot{\psi})^2}) \\ g_2 &= (2C_f - 2\frac{I_w}{R_{eff}^2}\ddot{x})\delta, \\ g_3 &= L_fg_2 + (-t_fC_f\frac{2t_f\dot{\psi}(\dot{y} + L_f\dot{\psi})}{\dot{x}^2 - (t_f\dot{\psi})^2})\delta + L_3(\ddot{y} + \dot{x}\dot{\psi}). \end{aligned} \tag{15}$$

The aim of the controller is to track a desired longitudinal speed while canceling the lateral displacement error with respect to a given reference trajectory. The control objective is then reached by generating a steering angle ($\delta$) and a driving/Braking wheels torque ($\tau_w$) that are suitable to track the reference trajectory defined by a trajectory planning module.

We define:

- $\dot{z}_1 = \dot{x}$,
- $\ddot{z}_2 = a_y = \ddot{y} + \dot{x}\dot{\psi}$.

where $\dot{z_1}$ represents the vehicle longitudinal speed, $\ddot{z}_2$ represents the vehicle lateral acceleration computed in the inertial frame.
To accomplish the control objective, we define two error signals as:

$$s_1 = \dot{e}_{z_1} = \dot{z}_1 - \dot{z}_1^* \tag{16}$$

$$s_2 = \dot{e}_{z_2} + \lambda e_{z_2} = \dot{z}_2 - \dot{z}_2^* + \lambda(z_2 - z_2^*),\ \lambda > 0 \tag{17}$$

where $s_1$ represents the vehicle longitudinal speed error and $s_2$ is function of the lateral displacements error ($e_{z_2}$) and its derivative computed at the vehicle center of gravity. The vectors with superscript ($*$) represent desired outputs.

The trajectory tracking is then guaranteed if and only if the longitudinal speed error and the lateral displacement error and its derivative ($\dot{e}_{z_1}$, $\dot{e}_{z_2}$ and $e_{z_2}$) converge in finite time to zero.

We make use of the concept of the control Lyapunov function (Attia et al. (2014)) to deduce the suitable control laws.

We define then a Lyapunov function as:

$$V = \frac{1}{2}s_1^2 + \frac{1}{2}\gamma s_2^2 \tag{18}$$

The derivative of this function is given by

$$\dot{V} = s_1\dot{s}_1 + \gamma s_2\dot{s}_2. \tag{19}$$

To ensure a stability convergence of $s_1$ and $s_2$, which guarantees the stability convergence of $e_{z_2}$, $\dot{e}_{z_2}$ and $\dot{e}_{z_1}$, we impose a negative variation of $V$ as:

$$\dot{V} = s_1\dot{s}_1 + \gamma s_2\dot{s}_2 = -K_1 s_1^2 - \gamma K_2 s_2^2 \tag{20}$$

where $K_1$ and $K_2$ represent the positive gains of this controller.

Equation (20) can be verified by taking:

$$s_1\dot{s_1} = -K_1 s_1^2. \tag{21}$$

$$s_2\dot{s_2} = -K_2 s_2^2. \tag{22}$$

Using (16) and (17), we have:

$$\ddot{x} = \ddot{z}_1^* - K_1\dot{e}_{z_1}. \tag{23}$$

$$\ddot{e}_{z_2} = -(K_2 + \lambda)\dot{e}_{z_2} - K_2\lambda e_{z_2}. \tag{24}$$

Assuming that the desired lateral acceleration of the vehicle on the reference trajectory can be written as $a_y^* = \dot{x}^2\rho_{ref}$, where $\rho_{ref}$ is the reference trajectory curvature, we have:

$$\ddot{e}_{z_2} = a_y - a_y^* = \ddot{y} + \dot{x}\dot{\psi} - \dot{x}^2\rho_{ref}$$

This yields:

$$\ddot{y} = \dot{x}^2\rho_{ref} - \dot{x}\dot{\psi} - (K_2 + \lambda)\dot{e}_{z_2} - K_2\lambda e_{z_2}. \tag{25}$$

Replacing (23) and (25) in the reduced system (14), we can deduce the longitudinal and the lateral commands as follows:

$$\begin{aligned}\tau_w = R_{eff}[&m_e\ddot{z}_1^* - m_e K_1\dot{e}_{z_1} - m\dot{y}\dot{\psi} \\ &+ L_3\dot{\psi}^2 + \delta(2C_f\delta - 2C_f\frac{\dot{x}(\dot{y} + L_f\dot{\psi})}{\dot{x}^2 - (t_f\dot{\psi})^2}) + F_{aero}]\end{aligned} \tag{26}$$

$$\begin{aligned}\delta = \frac{1}{(2C_f - 2\frac{I_w}{R_{eff}^2}\ddot{x})}[&m\dot{x}^2\rho_{ref} - m(K_2 + \lambda)\dot{e}_{z_2} - L_3\ddot{\psi} \\ &- mK_2\lambda e_{z_2} + 2C_f\frac{\dot{x}(\dot{y} + L_f\dot{\psi})}{\dot{x}^2 - (t_f\dot{\psi})^2} + 2C_r\frac{\dot{x}(\dot{y} - L_r\dot{\psi})}{\dot{x}^2 - (t_f\dot{\psi})^2}],\end{aligned} \tag{27}$$

To take into account the delay of the actuators, the lateral displacement error is computed at a look-ahead distance $L_s$ from the center of gravity of the vehicle (see Figure 5). $e_{z_2}$ is then given by:

$$e_{z_2} = z_2 - z_2^* + L_s(\psi - \psi^*).$$

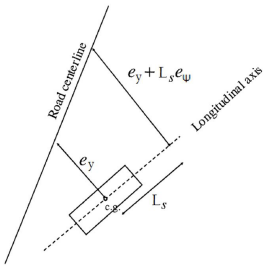


Fig. 5. Lateral error definition: $e_{z_2} = e_y + L_s e_\psi$, where $e_y = z_2 - z_2^*$ and $e_\psi = \psi - \psi^*$.

The lateral and the longitudinal dynamics of the vehicle are controlled simultaneously. Notice that the computation of the torque takes into consideration the lateral dynamics and the computation of the steering angle includes the longitudinal speed and acceleration values. The next section will present the results of the controller validation and some conclusions will be made.

### *3.2 Controller Validation*

To validate our control law, we make use of the real experimental data collected by performing several tests on the vehicle DYNA present in the Heudiasyc laboratory (Peugeot 308 sw). The collected data are considered as reference data that will be compared to those obtained by simulation on Matlab/simulink of the closed-loop system with the developed 4-wheels vehicle model and the developed controller. For the control laws, we use the gains $K_1 = 1.5$, $K_2 = 8$, $\lambda = 8$ and $L_s$ is fixed to $2m$ with the nominal vehicle parameters (see Table 2.2). Several tests have been done during normal driving conditions, and showed that the controlled vehicle is able to track the reference path with small error. We present in Figure 6,

a test that validates our controller during normal driving at high and varying speed and road curvature. The longitudinal desired speed varies between $5m/s$ and $25m/s$. Note that the maximal lateral acceleration is $5m/s^2$. In this scenario, the vehicle executes some maneuvers at low speed with large curvature and some at high speed with very low curvature. In other words, the vehicle navigates within a very narrow turn at low speed then it accelerates to reach a high speed on a low curvature road. The results presented in Figure 6 show that the vehicle is able to navigate with the desired speed while staying on the reference trajectory with a very small lateral displacement error ($< 3cm$ in our test conditions). The stability index is computed as in He et al. (2004), by $SI = 2.49\beta + 9.55\dot{\beta}$, where $\beta$ is the side slip angle at the center of gravity of the vehicle. Notice that, in this test, the hypothesis of small angles is not respected ($\delta$ reaches about 20°) and, despite this, the controller shows a good performance during these driving conditions. Moreover, the assumption of null slip ratio is not really respected in this driving scenario, since the slip ratio reaches in absolute value 0.02. Nevertheless, the control law proves to be robust to this assumption violation.

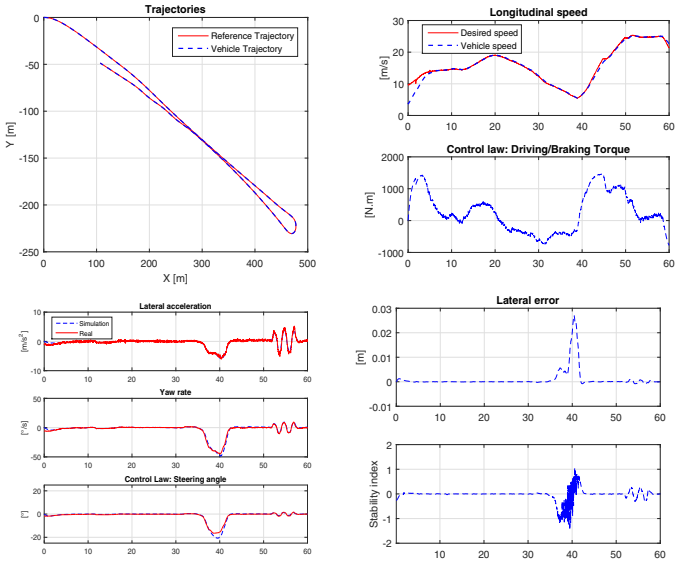


Fig. 6. a) Trajectories, b) Longitudinal speed and motor torque, c) Steering angle and lateral variables, d) Lateral displacement error and stability index

The robustness of the controlled system is then tested with respect to strongly non-linear maneuvers and uncertainties and disturbances encountered in automotive applications.

- Controller Robustness against strongly non-linear maneuvers:
  The test presented in Figure 7 shows a highly nonlinear maneuver. It consists on increasing progressively the vehicle speed while executing almost the same curvature (the radius is around 50m). The lateral acceleration and the longitudinal speed are increasing remarkably (the speed is increasing with a rate of $1m/s^2$ and the lateral acceleration reaches $8.5m/s^2$). This type of tests is used to evaluate the stability and the robustness of the controller against strong nonlinear dynamics. Figure 7.(b), 7.(a) and 7.(d) show that the vehicle succeeds to navigate with the desired speed and to track the desired trajectory (the lateral displacement error remains small) even in these conditions of navigation. In Figure 7.(c), the dynamic variables are very close to the measured ones, even at high lateral acceleration and a speed reaching about $57Km/h$. The results of this test show that the developed controller can ensure good performance even at the limit of stability.
  Notice that, the lateral error is increasing at $t = 14s$. This observation can be explained by the strong nonlinearity of the driving scenario at this point (the longitudinal and the lateral accelerations are very high at this point). To improve the robustness of the controller in such a situation, the tire/road forces modeling should be done by the mean of a nonlinear approach (piece-wise linear tire model, Dugoff model...).

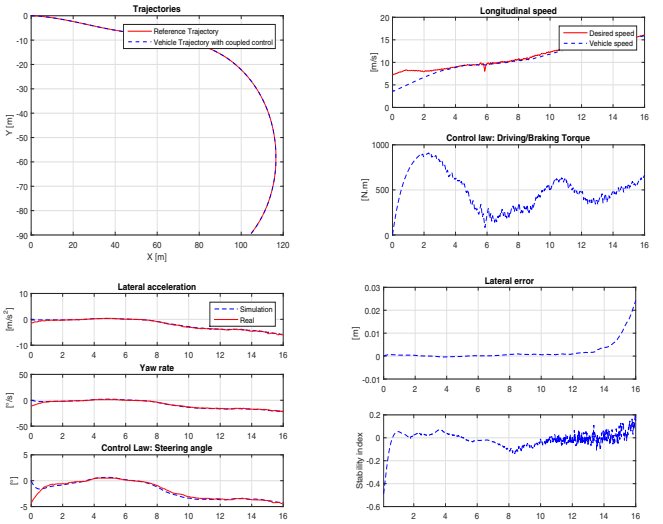


Fig. 7. a) Trajectories, b) Longitudinal speed and motor torque, c) Steering angle and lateral variables, d) Lateral displacement error and stability index

- Controller Robustness against parameters uncertainties:
  The robustness of the controller is evaluated over vehicle parameters uncertainty, especially the vehicle mass and the cornering stiffness. Actually, it is difficult to estimate accurately the stiffness of the tire since it is related to the road coefficient of friction, the type of the road, the vertical load, etc. Although, the vehicle mass could be poorly estimated or variable since it is dependent of the passengers and the amount of fuel. The controller robustness was evaluated for different parameters values. We present in Fig. 8, using the scenario presented in Figure 6, the lateral displacement errors and the longitudinal speeds for different stiffness and different mass (±30%). The results prove that the controller is able to follow the path with acceptable errors despite the parameters variations.

## 4. CONCLUSION

This paper presents a robotics approach used for the vehicle modeling. This formalism was used to elaborate a four wheeled vehicle model. The model was validated using Scaner-Studio simulator and the results show its validity for a large marge of driving conditions. Furthermore, a

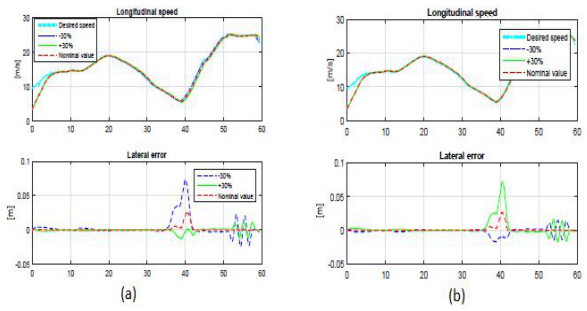


Fig. 8. Robustness against parameters uncertainties: a) vehicle mass uncertainties, b) cornering stiffness uncertainties.

coupled controller for the lateral and longitudinal dynamics was developed, based on this model. The controller was validated using experimental data collected on a vehicle in the Heudiasyc laboratory. The robustness of the control against parameters uncertainty was studied and the results show that the controller is efficient even with an uncertainty of ±30% on the studied parameters. We also studied its robustness against strong non-linearity and the controller was showing good performance even in the limits of stability. The short term outlook is to validate the controller on a robotized vehicle, while the long term outlooks will be the development of a planning module, that will generate a secure and feasible trajectory for the control level, based on several criteria related to the vehicle and its surrounding environment state.

## ACKNOWLEDGEMENTS

This work was carried out in the framework of the Labex MS2T, which was funded by the French Government, through the program Investments for the future managed by the National Agency for Research (Reference ANR-11-IDEX-0004-02) and the framework of the Equipex ROBOTEX (Reference ANR-10-EQPX-44-01), which was funded by the French Government, through the program Investments for the future managed by the National Agency for Research.

## REFERENCES

Ackermann, J., Guldner, J., Sienel, W., Steinhauser, R., and Utkin, V. (1995). Linear and nonlinear controller design for robust automatic steering. *Control Systems Technology, IEEE Transactions on*, 3(1), 132–143.

Attia, R., Orjuela, R., and Basset, M. (2014). Combined longitudinal and lateral control for automated vehicle guidance. *Vehicle Systems Dynamics*, 52(2), 261–279.

Baffet, G. (2007). *Développement et validation expérimentale dobservateurs des forces du contact pneumatique/chaussée dune automobile.* Ph.D. thesis, Compiègne.

Buehler, M., Iagnemma, K., and Singh, S. (2009). *The DARPA urban challenge: autonomous vehicles in city traffic*, volume 56. springer.

Dugoff, H., Fancher, P., and Segel, L. (1970). An analysis of tire traction properties and their influence on vehicle dynamic performance. Technical report, SAE Technical Paper.

He, J., Crolla, D., Levesley, M., and Manning, W. (2004). Integrated active steering and variable torque distribution control for improving vehicle handling and stability. Technical report, SAE Technical Paper.

Hollerbach, J.M. (1980). An iterative lagrangian formulation of manipulators dynamics and a comparative study of dynamics formulation complexity. In *IEEE Trans. on Systems, Man, and Cybernetics*.

Hooker, W. and Margulies, G. (1965). The dynamical attitude equations for a n-body satellite. In *The Journal of the Astronautical Sciences*.

Khalil, W. and Dombre, E. (2004). *Modeling, identification and control of robots.* Butterworth-Heinemann.

Khalil, W. and Kleinfinger, J. (1987). Minimum operations and minimum parameters of the dynamic model of tree structure robots. *IEEE J. Robotics and Automation*, 3(6), 517–526.

Khalil, W. and Kleinfinger, J.F. (1986). A new geometric notation for open and closed-loop robots. In *IEEE International Conference on Robotics and Automation*, volume 3.

Kiencke, U. and Nielsen, L. (2000). *Automotive Control Systems. For Engine, Driveline, and Vehicle.* Springer Verlag.

Luh, J., Walker, M., and Paul, R. (1980). On-line computational scheme for mechanical manipulators. *J. DYN. SYS. MEAS. and CONTR.*, 102, 69–76.

Maakaroun, S. (2011). *Modélisation et simulation dynamique d'un véhicule urbain innovant en utilisant le formalisme de la robotique.* Ph.D. thesis, Université Nantes Angers Le Mans.

Maakaroun, S., Khalil, W., Gautier, M., and Chevrel, P. (2014). Modeling and simulating a narrow tilting car using robotics formalism. *IEEE Transactions on Intelligent Transportation Systems*, 15(3), 1026–1038.

Mammar, S. and Netto, M. (2004). Integrated longitudinal and lateral control for vehicle low speed automation. *Proc. IEEE ICCA, Taiwan.*

Oktal (2016). *Driving simulation engine scaner. http://www.scanersimulation.com.*

Rajamani, R. (2006). *Vehicle Dynamics and Control.* Springer.

Rajamani, R., Tan, H.S., Law, B.K., and Zhang, W.B. (2000). Demonstration of integrated longitudinal and lateral control for the operation of automated vehicles in platoons. *Control Systems Technology, IEEE Transactions on*, 8(4), 695–708.

Renaud, M. (1975). *Contribution à l'étude de la modélisation et de la commande des systèmes mécaniques articulés.* Ph.D. thesis, UPS, Toulouse.

Sharp, R.S. (1971). The stability and control of motorcycles. *Mechanical Engineering Science*, 13(5), 316–326.

Tagne, G., Talj, R., and Charara, A. (2013). Higher-order sliding mode control for lateral dynamics of autonomous vehicles, with experimental validation. In *Intelligent Vehicles Symposium (IV), 2013 IEEE*, 678–683. IEEE.